IVYSPRING INTERNATIONAL PUBLISHER

International Journal of Medical Sciences

2026; 23(7): 2408-2422. doi: 10.7150/ijms.121198

Research Paper

Zingiber officinale Leaf Subcritical Water Extract Suppresses Adipogenesis and Lipogenesis in 3T3-L1 Adipocytes via the AMPK–SREBP-1c Signaling Pathway

Eun-Min Jun[1], Jong-Yeon Kim[2], Jeong-Sook Choe[3], Eun-Jung Park[1,2]✉, Hae-Jeung Lee[1,2,4,5]✉

1. Department of Food and Nutrition, Gachon University, Seongnam 13120, Republic of Korea.
2. Institute for Aging and Clinical Nutrition Research, Gachon University, Seongnam 13120, Republic of Korea.
3. Rural Development Administration, Jeonju 54875, Republic of Korea.
4. Department of Health Sciences and Technology, GAIHST, Gachon University, Incheon 21999, Republic of Korea.
5. Gachon Biomedical Convergence Institute, Gachon University Gil Medical Center, Incheon 21565, Republic of Korea.

✉ Corresponding authors: Hae-Jeung Lee, Ph. D., Professor, Department of Food and Nutrition, College of BioNano Technology, Gachon University, 1342 Seongnamdaero, Sujeong-gu, Seongnam-si, Gyeonggi-do 13120, Republic of Korea, Tel.: +82-31-750-5968; E-mail: skysea@gachon.ac.kr, skysea1010@gmail.com. Eun-Jung Park, Ph.D., Assistant Professor, Department of Food and Nutrition, College of BioNano Technology, Gachon University, 1342 Seongnamdaero, Sujeong-gu, Seongnam-si, Gyeonggi-do 13120, Republic of Korea, Tel: +82-31-724-4408; E-mail: ejpark@gachon.ac.kr.

Received: 2025.07.08; Accepted: 2026.05.26; Published: 2026.06.04

Abstract

Zingiber officinale, commonly known as ginger, has long been utilized as a medicinal plant due to its diverse pharmacological properties. However, research has predominantly focused on the rhizome, while the leaf is frequently regarded as a byproduct. In this study, we investigated the functional relevance of the ginger leaf, concentrating on the anti-obesity effects of ginger leaf subcritical water extract (GLE) and the underlying mechanisms in 3T3-L1 adipocytes. GLE reduced lipid accumulation in a concentration-dependent manner on day 7 of differentiation and suppressed the expression of adipogenesis-associated factors, including CCAAT/enhancer-binding protein α (C/EBPα), peroxisome proliferator-activated receptor γ, fatty acid binding protein 4, and lipoprotein lipase on both days 2 and 7. GLE also modulated early adipogenesis by inhibiting p38 phosphorylation and downregulating C/EBPβ expression at 4 h of differentiation. Additionally, GLE decreased the expression of acetyl-CoA carboxylase, fatty acid synthase, and stearoyl-CoA desaturase 1—key enzymes involved in lipogenesis—from the early stages of adipocyte differentiation. Furthermore, GLE directly phosphorylated adenosine monophosphate-activated protein kinase (AMPK), leading to inhibition of the expression of sterol regulatory element-binding protein-1c (SREBP-1c), an upstream regulator of both adipogenesis and lipogenesis. In summary, GLE exerted anti-obesity effects in 3T3-L1 adipocytes by inhibiting the transcriptional activation of adipogenic and lipogenic regulators during the early stage of differentiation, and maintaining their downregulation at later stages, and it was found to be mediated by the AMPK–SREBP-1c signaling pathway.

Keywords: Ginger leaf; Subcritical water; 3T3-L1; Adipogenesis; Lipogenesis; AMPK–SREBP-1c

Introduction

Obesity is commonly described as excessive body fat accumulation, and weight gain occurs when energy intake chronically exceeds energy expenditure [1]. Dysfunctional and hypertrophic adipose tissue can secrete adipose-derived factors and contribute to obesity-associated complications, including type 2 diabetes, cancer, and cardiovascular diseases [2, 3]. The prevalence of obesity has risen markedly worldwide [4, 5], particularly in Korea, where obesity prevalence has increased 1.27-fold since 2012 [6]. Consequently, interest in pharmacotherapy for obesity treatment is increasing [7]. However, many anti-obesity drugs have been withdrawn due to severe adverse effects [8]. Consequently, the demand for natural products with lower toxicity, such as herbal remedies, is expanding.

Zingiber officinale, commonly known as ginger, is a perennial herb of the Zingiberaceae family and contains approximately 80–90 non-volatile bioactive compounds, including gingerol, shogaol, quercetin, ferulic acid, rutin, and catechin [9-11]. These compounds exhibit a broad spectrum of pharmacological activities, such as anti-obesity, antioxidant, and anti-inflammatory effects, and ginger has been used medicinally since ancient times [12]. For example, boiled ginger improved the lipid profile in rats fed a high-cholesterol diet [13], and another study indicated that ginger may prevent obesity via multiple mechanisms, including thermogenesis, lipolysis, lipogenesis, fat absorption, and controlling appetite [14]. Notably, recent research demonstrated that among ginger plant parts, the leaf contains the highest levels of polyphenols such as rutin, quercetin-3-glucoside, quercetin, and kaempferol [15]. Despite this, most studies have concentrated on the rhizome, while the leaf is typically discarded during cultivation and remains underutilized despite its biofunctional potential [16]. Therefore, investigating the biofunctional properties of ginger leaves and identifying novel applications is warranted.

The growth and maturation of preadipocytes proceed through sequential processes, including adipogenesis, lipogenesis, and lipid accumulation. In particular, adipogenesis proceeds through several stages. Following hormonal stimulation, preadipocytes undergo growth arrest and several rounds of cell division, which is mitotic clonal expansion (MCE; 0–2 days) [17]. Upon completion of MCE, cells enter terminal differentiation (2–7 days), during which late adipogenic markers, along with lipogenic genes, are upregulated [18-21]. Adenosine monophosphate-activated protein kinase (AMPK) and sterol regulatory element-binding protein 1c (SREBP-1c) act as upstream regulators of these processes. SREBPs serve as master regulators of lipid biosynthesis by controlling enzymes involved in the synthesis of cholesterol, fatty acids (FAs), and triglycerides (TGs) [22, 23]. In mammals, SREBPs consist primarily of isoforms SREBP-1a, -1c, and -2, with SREBP-1c predominantly expressed in liver and adipose tissue [24]. AMPK is present in all tissues and maintains energy homeostasis by regulating ATP production and consumption [25]. In 3T3-L1 cells, AMPK directly phosphorylates SREBP-1c at Ser372, inhibiting its proteolytic maturation and nuclear translocation [26]. This suggests that the inhibition of lipid biosynthesis through the modulation of the AMPK–SREBP-1c signaling pathway may represent a promising therapeutic approach for obesity treatment.

In addition to these metabolic signaling pathways, oxidative stress is also considered a key factor influencing obesity. Oxidative stress has been implicated in obesity because excessive reactive oxygen species (ROS) can activate signaling pathways that promote adipogenesis and lipogenesis through regulators such as sterol regulatory element-binding protein-1c (SREBP-1c), CCAAT/enhancer-binding protein alpha (C/EBPα), and peroxisome proliferator-activated receptor gamma (PPARγ) [27, 28]. Consequently, compounds with high antioxidant capacity have been shown to attenuate these processes, representing a complementary strategy for anti-obesity treatment [27, 29].

In this study, we evaluated the anti-obesity effects of ginger leaf subcritical water extract (GLE), highlighting its potential as a therapeutic agent for obesity. Multiple natural compounds have been reported to inhibit adipogenesis in a stage-dependent manner [30, 31]. Based on these findings, we investigated the timing of GLE effects by analyzing expression levels of key markers at early (4 h and day 2) and terminal (day 7) stages of differentiation. Additionally, the molecular mechanisms underlying GLE effects were examined, with particular emphasis on the AMPK–SREBP-1c signaling pathway.

Materials and Methods

Preparation of GLE

Ginger leaves were obtained from a commercial supplier in Seosan, Chungcheongnam-do, Korea, and were provided as a homogeneous batch suitable for extraction. The leaves were dried in a 60 °C hot air dryer for 12 h, ground, and sieved through a 30-mesh to obtain a dry powder. Prior to extraction, the powder was spread on a petri dish and further dried at 60–70 °C for 24 h. A mixture of 1 g of ginger leaf powder and 2 g of diatomaceous earth was packed into a 22 mL stainless-steel extraction cell (23 mm i.d. × 50 mm, Dionex, Sunnyvale, CA, USA). Subcritical water extraction was carried out at 130 °C for 10 min under 10 MPa using a Dionex™ ASE™ 350 Accelerated Solvent Extractor (Dionex, Sunnyvale, CA, USA) with distilled water. The extract was centrifuged at 4,000 rpm for 25 min, and the supernatant was collected, frozen in an ultra-low-temperature freezer for 24 h, and lyophilized for 48 h using a freeze-dryer.

Quantitative analysis of GLE bioactive compounds using high-performance liquid chromatography (HPLC)

HPLC analysis was performed using an Agilent 1100-diode array detector system. Separation was carried out on an Imtakt Cadenza CD-C18 column (4.6 × 250 mm, 3 μm) maintained at 35°C. A gradient

system composed of formic acid in water (mobile phase A) and acetonitrile (mobile phase B) was delivered at a flow rate of 0.7 mL/min. The gradient elution program was as follows: 10% B (0–5 and 60–65 min), 80% B (5–55 min), 95% B (55–60 min). The injection volume was 10 µL, and the detection was performed at 350 nm.

ABTS radical scavenging assay

A 7 mM solution of 2,2′-azino-bis(3-ethylbenzothiazoline-6-sulfonic acid) (ABTS; Sigma-Aldrich, MO, USA) was mixed with a 2.45 mM solution of potassium persulfate and incubated in the dark for 24 h. Subsequently, 150 µL of the ABTS solution was added to 50 µL of ascorbic acid (1.56–20 µg/mL) or GLE (12.5–1,000 µg/mL) at each concentration in a 96-well plate. The reaction was carried out in the dark for 5 min, and absorbance was measured at 734 nm using an Epoch microplate spectrophotometer (BioTek Instruments, Winooski, VT, USA). ABTS radical scavenging ability was calculated using the following formula:

$$\text{Scavenging activity (\%)} = \left(\frac{A_B - A_S}{A_B}\right) \times 100$$

where A_B and A_S represent the absorbance values of the blank and sample, respectively.

Cell culture and differentiation

3T3-L1 cells were obtained from the American Type Culture Collection (ATCC; Manassas, VA, USA). 3T3-L1 preadipocytes were cultured in Dulbecco's modified Eagle's medium (DMEM; Corning, NY, USA) supplemented with 10% bovine calf serum (Gibco, Grand Island, NY, USA) and 1% antibiotic-antimycotic solution (Gibco, Grand Island, NY, USA) in a 5% CO_2 incubator at 37 °C.

To induce differentiation, 3T3-L1 preadipocytes were seeded at a density of 5 × 10^4 cells/mL and maintained until reaching confluence. The cells were then cultured in DMEM containing 10% fetal bovine serum (FBS; Gibco, Grand Island, NY, USA), 0.5 mM 1-methyl-3-isobutylxanthine (Sigma-Aldrich, MO, USA), 1 µM dexamethasone (Sigma-Aldrich, MO, USA), and 10 µg/mL insulin (Gibco, Grand Island, NY, USA) for 3 days. This was followed by a 2-day incubation in DMEM containing 10% FBS and 10 µg/mL insulin. From day 5 onward, the medium was replaced with DMEM containing 10% FBS and maintained until day 7. GLE was administered during the differentiation period.

Cell viability assay

Cell viability was evaluated using the 3-(4,5-dimethylthiazol-2-yl)-2,5-diphenyltetrazolium bromide (MTT; Sigma-Aldrich, MO, USA) assay. 3T3-L1 preadipocytes were seeded at a density of 1 × 10^5 cells/mL in 96-well plates and incubated for 24 h, followed by treatment with GLE at six concentrations (0, 50, 100, 200, 400, and 800 µg/mL) for 72 h. Medium containing 0.5 mg/mL MTT solution was added to each well and incubated at 37°C for 1 h. After aspirating the medium, formazan crystals were solubilized in 100 µL of dimethyl sulfoxide, and absorbance was measured at 540 nm. 3T3-L1 adipocytes were differentiated for 7 days as previously described and subsequently subjected to the MTT assay using the same protocol.

Oil red O staining

Lipid accumulation was assessed by Oil Red O staining. 3T3-L1 cells were seeded at a density of 5 × 10^4 cells/mL in 6-well plates, differentiated for 7 days, and fixed with 4% paraformaldehyde (iNtRON Biotechnology, Gyeonggi-do, Korea). Oil Red O solution (Sigma-Aldrich, MO, USA), diluted in a 3:2 ratio with distilled water, was used to stain the cells. The stained lipid droplets of the cells were washed and imaged using an ECLIPSE Ts2 microscope (Nikon, Tokyo, Japan). After capturing the image, the staining dye from the cells was then eluted using 100% isopropanol (Sigma-Aldrich, MO, USA), and absorbance was measured at 500 nm using a microplate spectrophotometer.

Quantitative reverse transcription polymerase chain reaction (qRT-PCR) analysis

Total mRNA was extracted from 3T3-L1 cells using the Total RNA Extraction Kit (iNtRON Biotechnology, Gyeonggi-do, Korea). mRNA quantified at 50 ng/µL was mixed with GoScript™ Reverse Transcriptase Mix (Promega, Madison, WI, USA) and reverse transcribed into cDNA using the TaKaRa PCR Thermal Cycler Dice® Touch (Takara Bio, Shiga, Japan). The synthesized cDNA was mixed with TB Green® Premix Ex Taq™ II (Takara Bio, Shiga, Japan) and forward and reverse primers (Table 1), followed by qRT-PCR using the QuantStudio 3 Real-Time PCR Instrument (Applied Biosystems, Foster City, CA, USA). Relative mRNA expression was determined using the $2^{-\Delta\Delta}$CT method.

Western blot analysis

3T3-L1 cells were lysed in RIPA buffer (iNtRON Biotechnology, Gyeonggi-do, Korea) containing Halt™ phosphatase inhibitor cocktail (Thermo fisher scientific, Waltham, MA, USA) and a protease inhibitor (Sigma-Aldrich, MO, USA). After incubating for 10 min at 4 °C, the lysates were centrifuged at 13,000 rpm for 10 min. The supernatant was collected,

and the protein was quantified using the TaKaRa BCA Protein Assay Kit (Takara Bio, Shiga, Japan). 40 μg of protein was electrophoresed on a sodium dodecyl sulfate-polyacrylamide gel and transferred to a polyvinylidene difluoride membrane. The membrane was blocked with 5% skim milk (BD Difco, Sparks, MD, USA) for 1 h and incubated with primary antibody (Table 2) at 4 °C overnight. The membranes were then incubated with horseradish peroxidase-conjugated secondary antibodies (Promega, Madison, WI, USA) for 1 h at room temperature. Protein bands were detected using Western Blot Detection System (iNtRON Biotechnology, Gyeonggi-do, Korea) and quantified with ImageQuant™ LAS 500 system (GE Healthcare Life Sciences, Little Chalfont, UK).

Statistical analysis

All data are expressed as the mean ± standard deviation of at least three independent experiments. Statistical analysis was conducted using GraphPad Prism 10 software (GraphPad Software Inc., San Diego, CA, USA). Differences between two groups were evaluated using the Student's *t*-test, while comparisons among more than two groups were analyzed using one-way analysis of variance (ANOVA) followed by Tukey's post hoc test. A p-value < 0.05 was considered statistically significant.

Results

Phytochemical profile and ABTS radical scavenging activity of GLE

GLE contained two major phenolic compounds, ferulic acid (2.27 mg/g) and rutin (1.91 mg/g), as identified by HPLC analysis (Fig. 1). Given the documented antioxidant properties of these phenolics, the antioxidant capacity of GLE was further assessed using the ABTS radical-scavenging assay (Fig. S1). GLE exhibited a concentration-dependent scavenging effect, with approximately 90% radical scavenging at concentrations above 500 μg/mL. The IC_{50} value of GLE was 168.86 ± 8.98 μg/mL, whereas that of ascorbic acid, used as a positive control, was 8.40 ± 0.01 μg/mL.

Effects of GLE on cell viability and lipid accumulation in 3T3-L1 cells

The protocol for the differentiation of 3T3-L1 preadipocytes into adipocytes is shown in Fig. 2A. 3T3-L1 preadipocytes and adipocytes were treated with GLE at concentrations of 50, 100, 200, 400, and 800 μg/mL to determine the non-cytotoxic concentration. GLE showed no cytotoxicity at concentrations up to 800 μg/mL in both preadipocytes and adipocytes (Fig. 2B, C). Differentiated 3T3-L1 cells were stained with Oil Red O to assess the effect of GLE treatment on lipid accumulation. Compared to untreated cells, all GLE-treated groups showed a significant reduction in lipid accumulation, with the most pronounced reduction observed at 800 μg/mL (Fig. 2D, E). These findings suggest that GLE reduces lipid production and accumulation in 3T3-L1 cells.

Table 1. Primer sequences used for qRT-PCR analysis

Gene	Primer sequences (5′–3′)	Accession Number
Srebf1	F: TGTTGGCATCCTGCTATCTG R: AGGGAAAGCTTTGGGGTCTA	BC056922.1
Acaca	F: GCGTCGGGTAGATCCAGTT R: CTCAGTGGGGCTTAGCTCTG	NM_133360.3
Fasn	F: TTGCTGGCACTACAGAATGC R: AACAGCCTCAGAGCGACAAT	NM_007988.3
Scd1	F: TTCCCTCCTGCAAGCTCTAC R: CAGAGCGCTGGTCATGTAGT	NM_009127.4
Pparg	F: TTTTCAAGGGTGCCAGTTT R: AATCCTTGGCCCTCTGAGAT	U01841.1
Cebpa	F: TTACAACAGGCCAGGTTTCC R: GGCTGGCGACATACAGTACA	NM_007678.4
Fabp4	F: TCACCTGGAAGACAGCTCCT R: AATCCCCATTTACGCTGATG	NM_001409514.1
Lpl	F: TCCAAGGAAGCCTTTGAGAA R: CCATCCTCAGTCCCAGAAAA	NM_008509.2
Cebpb	F: CCAAGAAGACGGTGGACAA R: CAAGTTCCGCAGGGTGCT	NM_001287739.1
Actb	F: CCACAGCTGAGAGGAAATC R: AAGGAAGGCTGGAAAAGAGC	NM_007393.5

Srebf1, sterol regulatory element-binding protein 1; *Acaca*, acetyl-CoA carboxylase alpha; *Fasn*, fatty acid synthase; *Scd1*, stearoyl-CoA desaturase 1; *Pparg*, peroxisome proliferator-activated receptor gamma; *Cebpa*, CCAAT/enhancer-binding protein alpha; *Fabp4*, fatty acid-binding protein 4; *Lpl*, lipoprotein lipase; *Cebpb*, CCAAT/enhancer-binding protein beta; *Actb*, beta-actin

Table 2. Antibodies used for western blot analysis

Antibody	Source	Manufacturer	Catalog Number
C/EBPβ	Rabbit	Cell Signaling Technology	3087S
C/EBPα	Rabbit	Cell Signaling Technology	2295S
PPARγ	Rabbit	Cell Signaling Technology	2435S
FABP4	Rabbit	Cell Signaling Technology	2120S
Phospho-ACC	Rabbit	Cell Signaling Technology	3661S
ACC	Rabbit	Cell Signaling Technology	3662S
FAS	Mouse	Santa Cruz	SC-48357
Phospho-AMPK	Rabbit	Cell Signaling Technology	2535S
AMPK	Rabbit	Cell Signaling Technology	2532S
SREBP-1c	Mouse	Santa Cruz	SC-13551
Phospho-p38	Rabbit	Cell Signaling Technology	4511S
p38	Rabbit	Cell Signaling Technology	8690S
Phospho-JNK	Rabbit	Cell Signaling Technology	4668S
JNK	Rabbit	Cell Signaling Technology	9252S
β-actin	Mouse	Cell Signaling Technology	3700S

C/EBP, CCAAT/enhancer-binding protein; PPARγ, peroxisome proliferator-activated receptor gamma; FABP4, fatty acid-binding protein 4; ACC, acetyl-CoA carboxylase; FAS, fatty acid synthase; AMPK, adenosine monophosphate-activated protein kinase; FAS, fatty acid synthase; SREBP-1c, sterol regulatory element-binding protein 1c; JNK, c-Jun N-terminal kinase; β-actin, beta-actin

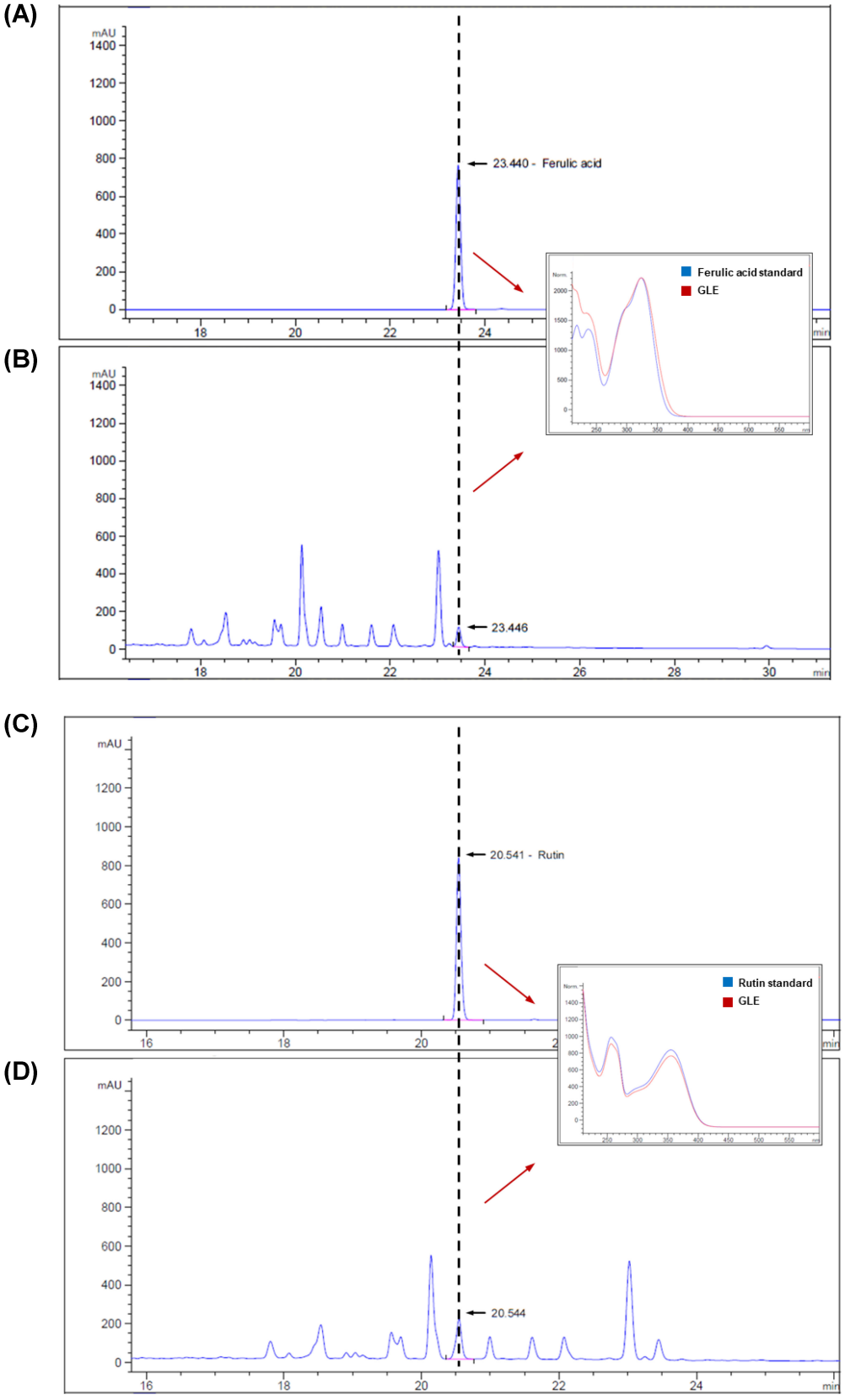

Figure 1. Quantification of bioactive compound in GLE using high-performance liquid chromatography (HPLC). (A) Ferulic acid standard (0.451 mg/mL) and (B) GLE sample. (C) Rutin standard (0.153 mg/mL) and (D) GLE sample. GLE, ginger leaf subcritical water extract

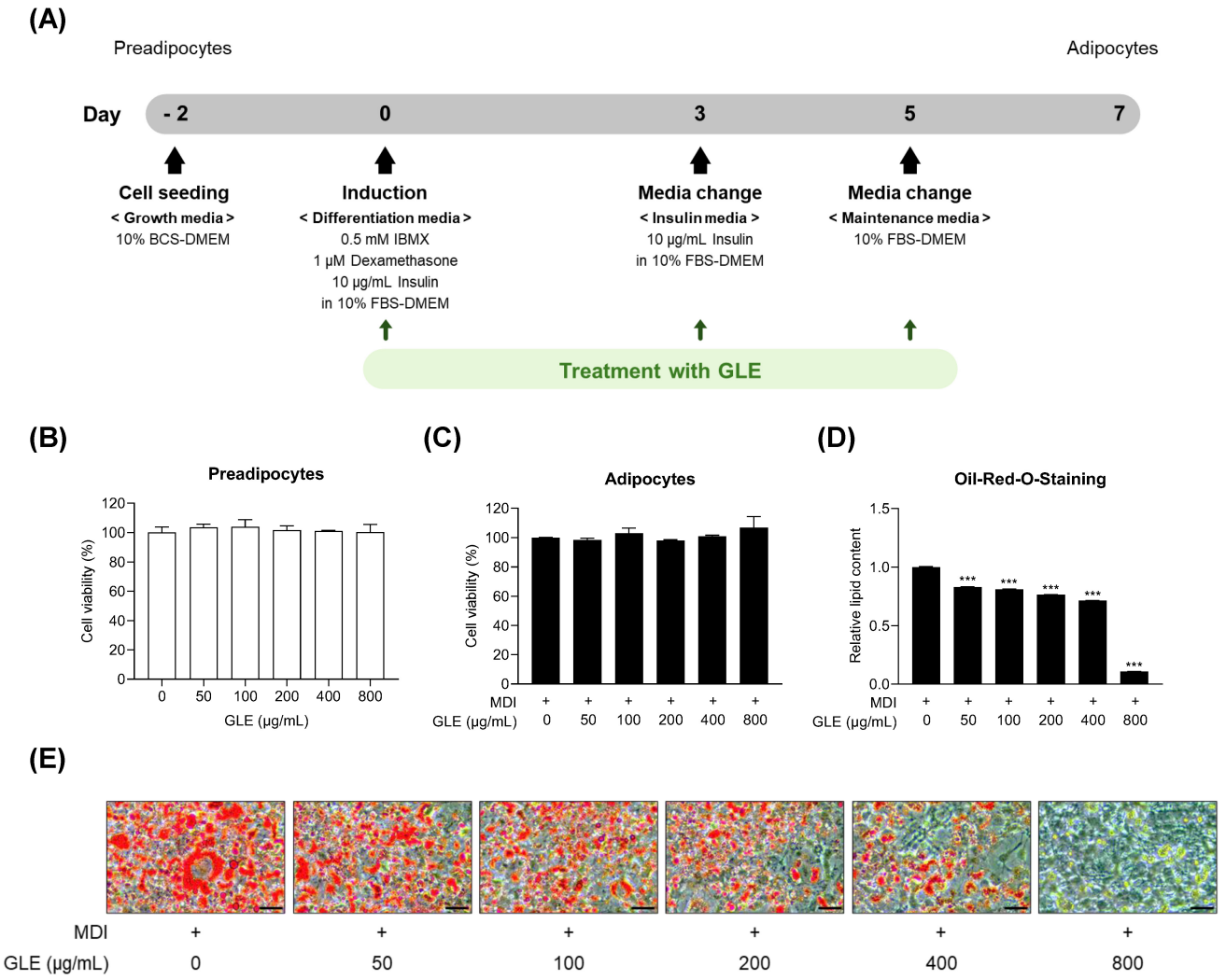

Figure 2. Effects of GLE on cell viability and lipid accumulation in 3T3-L1. (A) Experimental design for the differentiation of 3T3-L1 preadipocytes. Cell viability of (B) 3T3-L1 preadipocytes after 72 h and (C) 3T3-L1 adipocytes after 7 d. (D) Quantification of Oil Red O-stained lipid droplets. (E) Representative images of Oil Red O staining (200×; scale bar = 50 μm). Data are presented as the mean ± SD. ***$p < 0.001$ vs. 0 μg/mL. GLE, ginger leaf subcritical water extract

Effects of GLE on adipogenesis in 3T3-L1 adipocytes

To assess whether GLE reduces adipogenesis in 3T3-L1 adipocytes, qRT-PCR and western blot analyses were performed. GLE treatment decreased the mRNA expression levels of C/EBPα, PPARγ, fatty acid binding protein 4 (FABP4), and lipoprotein lipase (LPL) on days 2 and 7 (Fig. 3A–D). In addition, GLE treatment reduced C/EBPβ protein expression at 4 h (Fig. 3E). Protein expression levels of C/EBPα, PPARγ, and FABP4 were also decreased by GLE treatment on days 2 and 7 (Fig. 3F). These results indicate that GLE inhibits C/EBPβ expression during the early stage of differentiation in 3T3-L1 cells, which in turn downregulates the expression of C/EBPα, PPARγ, FABP4, and LPL.

Effects of GLE on lipogenesis in 3T3-L1 adipocytes

To assess the effect of GLE on lipogenesis, the expression of lipogenesis-related factors was evaluated on days 2 and 7 of differentiation in 3T3-L1 adipocytes. GLE decreased the mRNA expression levels of acetyl-CoA carboxylase (ACC), fatty acid synthase (FAS), and stearoyl-CoA desaturase 1 (SCD1) (Fig. 4A–C). Western blot analysis revealed that GLE inhibited FAS protein expression, increased ACC phosphorylation, and decreased total ACC levels (Fig. 4D). These results indicate that GLE inhibited lipogenesis by modulating the expression of lipogenesis-related genes from day 2 of differentiation.

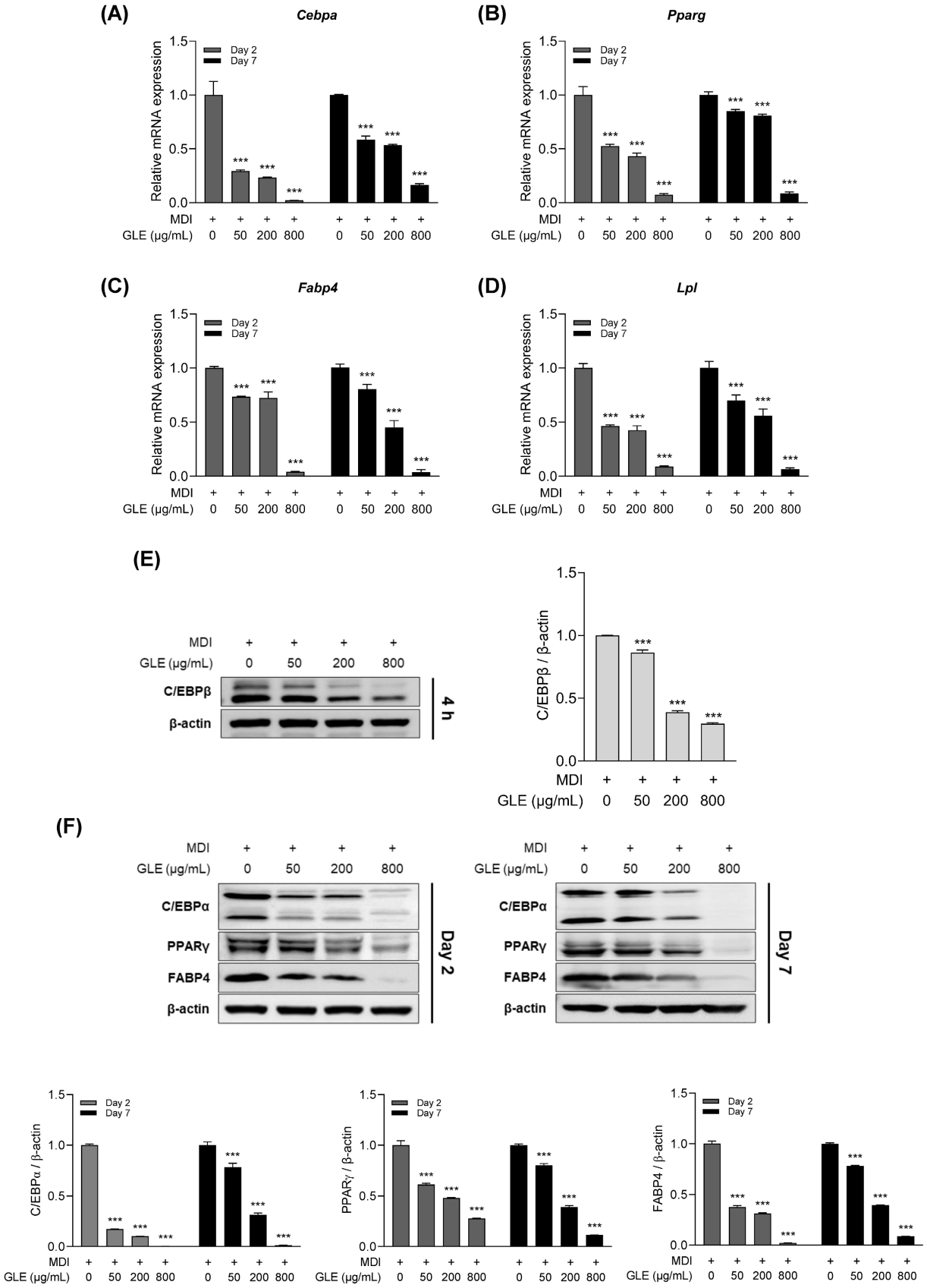

Figure 3. Effects of GLE on adipogenesis in 3T3-L1 adipocytes. Relative mRNA expression levels of (A) *Cebpa*, (B) *Pparg*, (C) *Fabp4*, and (D) *Lpl* on days 2 and 7. (E) Representative western blot images and quantification of C/EBPβ at 4 h. (F) Western blot images and quantification of C/EBPα, PPARγ, and FABP4 on days 2 and 7. Data are presented as the mean ± SD. ***$p < 0.001$ vs. 0 μg/mL. GLE, ginger leaf subcritical water extract

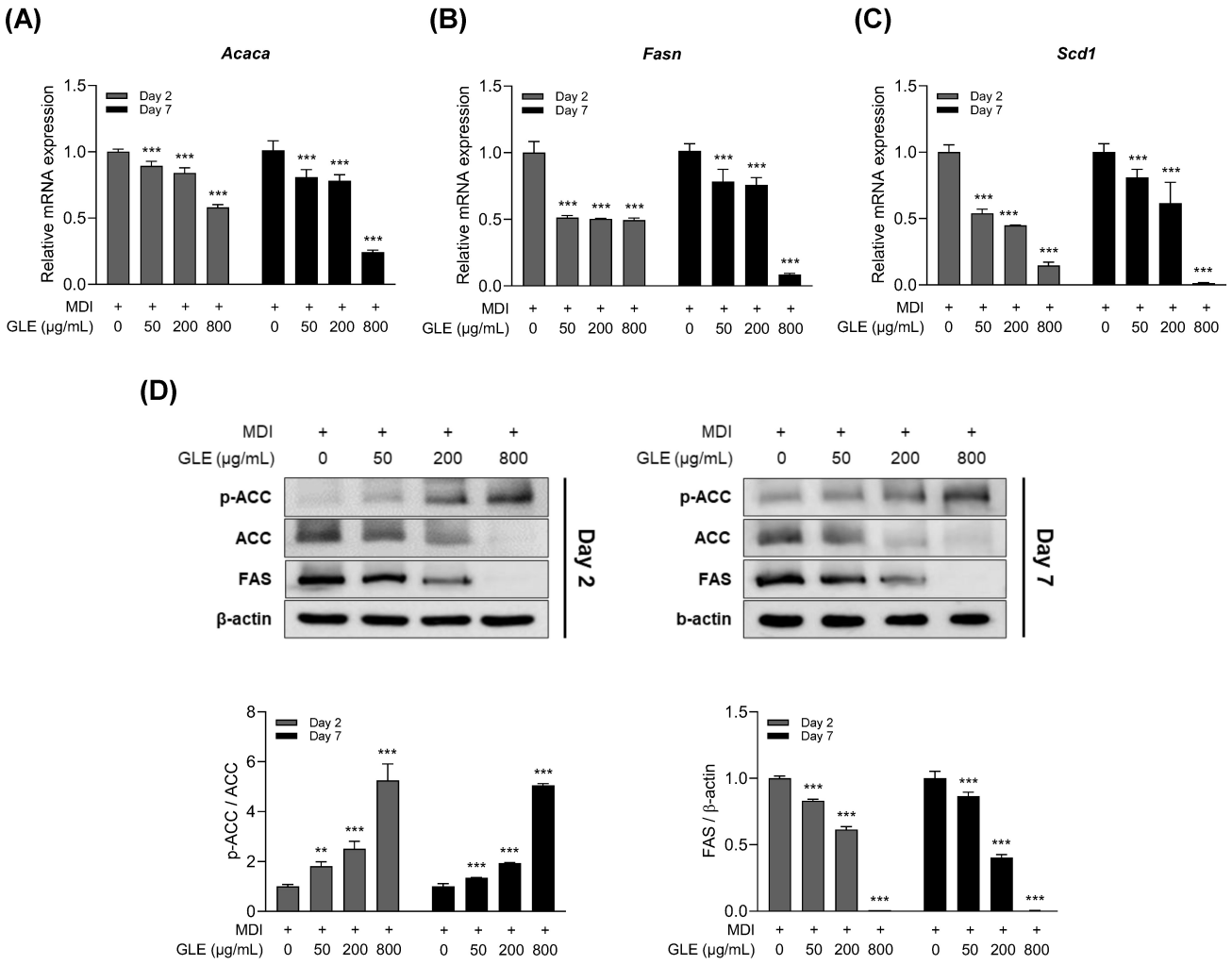

Figure 4. Effects of GLE on lipogenesis in 3T3-L1 adipocytes. Relative mRNA expression levels of (A) *Acaca*, (B) *Fasn*, and (C) *Scd1* on days 2 and 7. (D) Representative western blot images and quantification of ACC and FAS protein levels on days 2 and 7. Data are presented as the mean ± SD. $^{**}p < 0.01$, $^{***}p < 0.001$ vs. 0 μg/mL. GLE, ginger leaf subcritical water extract

Effects of GLE on the AMPK–SREBP-1c signaling pathway in 3T3-L1 adipocytes

To determine whether AMPK and SREBP-1c, which are implicated in the regulation of adipogenesis and lipogenesis, mediate the anti-obesity effects of GLE, expression levels were evaluated on days 2 and 7 (Fig. 5A, B). GLE reduced the mRNA expression of SREBP-1c and decreased both the precursor and mature forms of the SREBP-1c protein. In addition, GLE upregulated AMPK phosphorylation.

To further investigate whether GLE mediates its effects through the AMPK–SREBP-1c signaling pathway, 3T3-L1 cells were treated with GLE in the presence of AMPK modulators, including the AMPK inhibitor compound C and the AMPK activator AICAR. GLE increased phosphorylation of AMPK and ACC and decreased SREBP-1c expression. This effect was reversed by co-treatment with compound C (Fig. 6). Furthermore, the GLE-induced increase in AMPK and ACC phosphorylation and reduction in SREBP-1c expression were enhanced by co-treatment with AICAR. GLE also significantly reversed lipid accumulation and the expression of adipogenic markers such as C/EBPα, PPARγ, and FABP4 when co-treated with Compound C (Fig. S2). These findings indicate that GLE inhibits adipogenesis, lipogenesis, and lipid accumulation via the AMPK–SREBP-1c signaling pathway in 3T3-L1 adipocytes.

Effects of GLE on phosphorylation of MAPKs in 3T3-L1 adipocytes

Mitogen-activated protein kinases (MAPKs) regulate adipogenesis- and lipogenesis-related factors through multiple signaling pathways [32, 33]. To evaluate the effect of GLE on MAPK activity, phosphorylation levels of key MAPKs were assessed. GLE treatment decreased the phosphorylation of p38

and c-Jun N-terminal kinase (JNK) in a concentration-dependent manner at both 4 h and day 2 (Fig. 7). These results suggest that GLE reduces p38 and JNK phosphorylation from the early stages of differentiation, indicating that GLE-mediated MAPKs inhibition may modulate the activity of key factors involved in adipogenesis and lipogenesis.

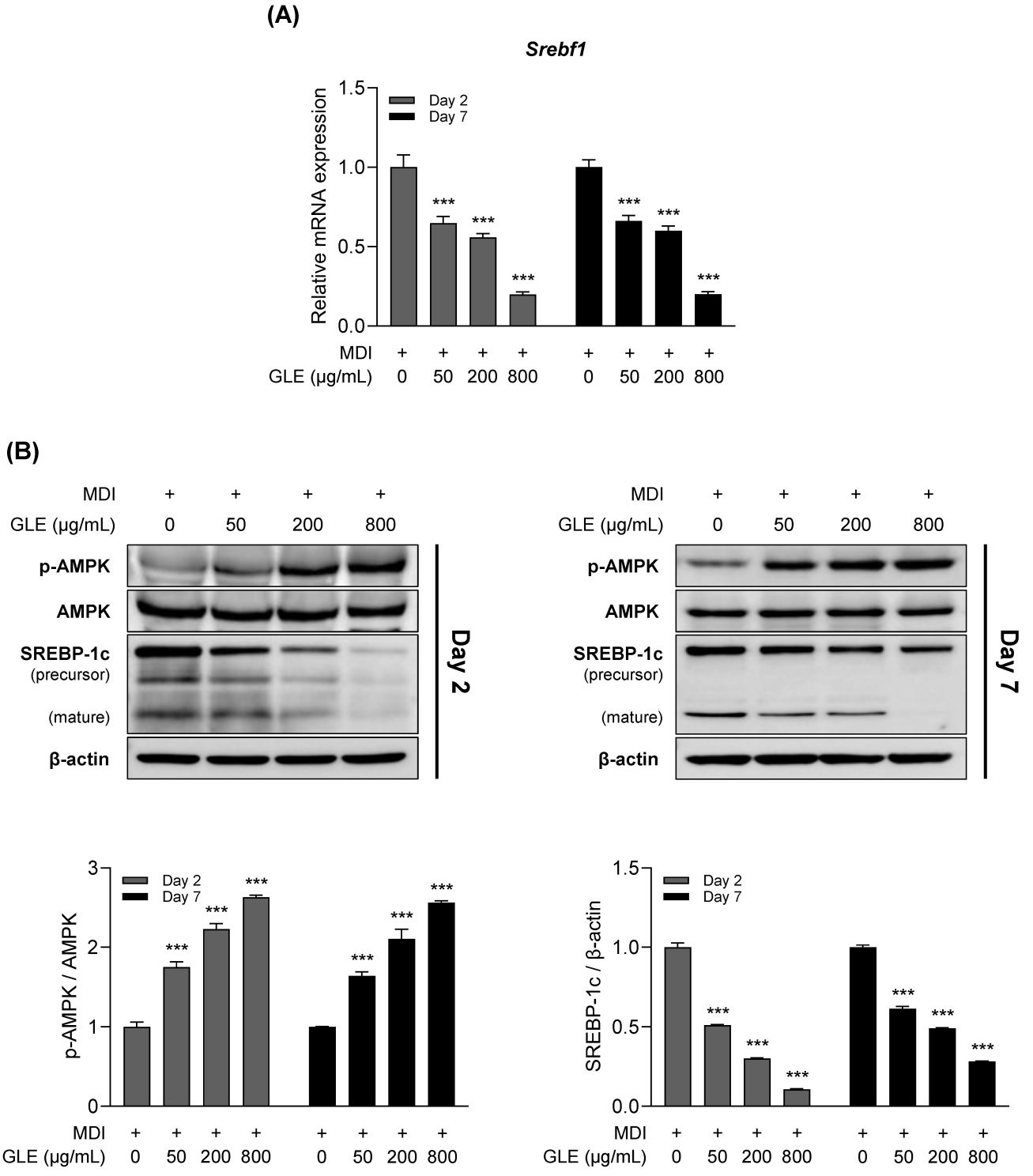

Figure 5. Effects of GLE on AMPK and SREBP-1c expression in 3T3-L1 adipocytes. (A) Relative mRNA expression of *Srebf1*. (B) Western blot images and quantification of p-AMPK/AMPK and SREBP-1c protein levels on days 2 and 7. Data are presented as the mean ± SD. ***$p < 0.001$ vs. 0 μg/mL. GLE, ginger leaf subcritical water extract

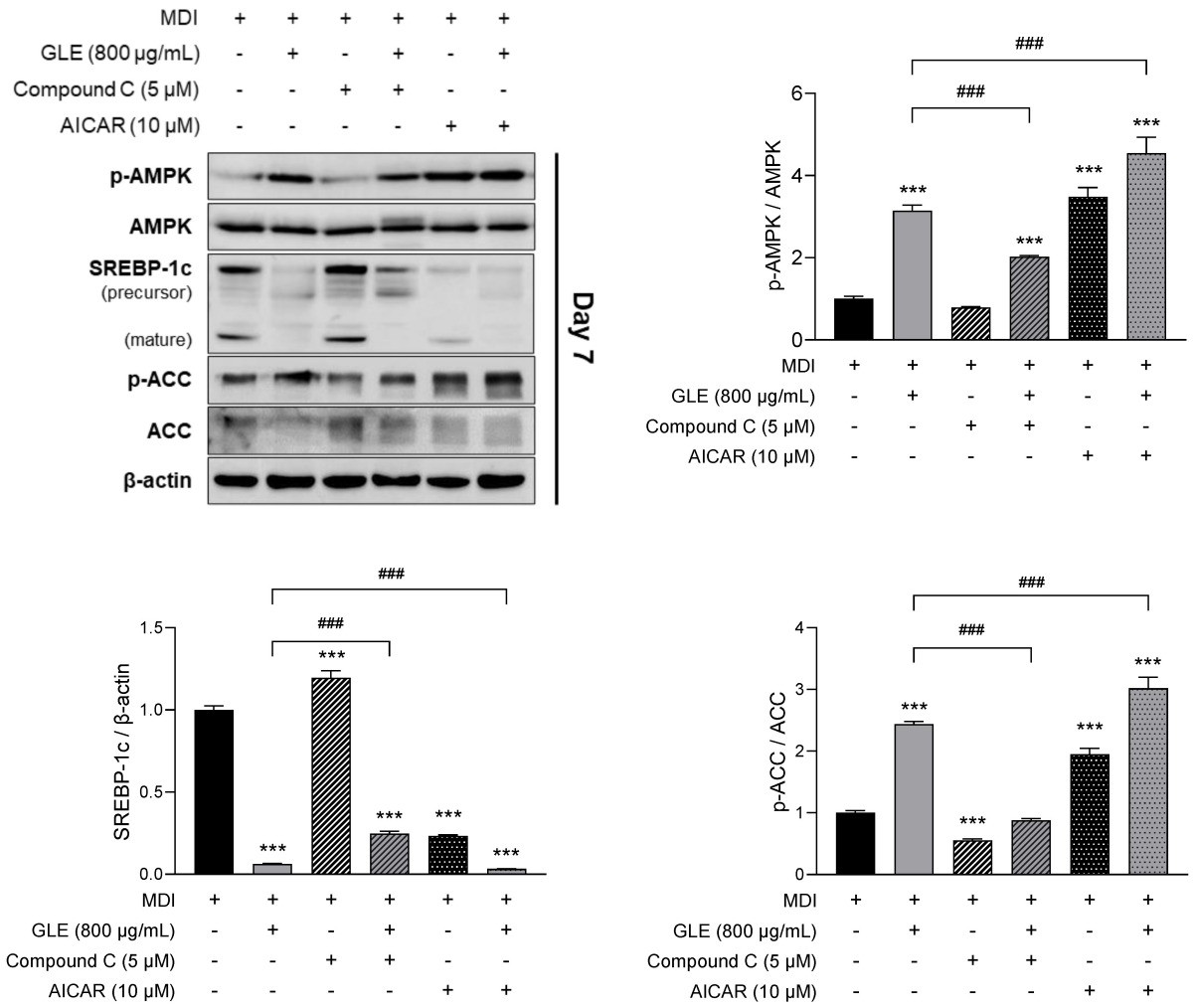

Figure 6. Effects of GLE on the AMPK–SREBP-1c signaling pathway in 3T3-L1 adipocytes. Western blot images and quantification of p-AMPK/AMPK, SREBP-1c, and p-ACC/ACC protein levels treated with or without Compound C (AMPK inhibitor), or AICAR (AMPK activator) on day 7. Data are presented as the mean ± SD. $^{***}p < 0.001$ vs. MDI; $^{###}p < 0.001$ vs. GLE. GLE, ginger leaf subcritical water extract

Discussion

Obesity is a chronic disease characterized by an excessive accumulation of adipose tissue resulting from both hyperplasia and hypertrophy of adipocytes [34]. It is not merely an individual condition but persists across the lifespan and transgenerationally [35]. However, long-term drug treatment is associated with risks of dependence and adverse effects [36]. Consequently, natural products have attracted interest as potentially safer therapeutic alternatives for managing obesity.

Among the parts of ginger, the rhizome has been extensively studied and is known to exhibit various bioactive properties [37], whereas the leaf is considered a by-product and has not been fully studied. Interestingly, previous studies comparing different parts of ginger have reported that the leaf exhibits the highest antioxidant capacity and polyphenol content among the rhizome, leaf, and flower [15, 38]. This suggests the pharmacological potential of the ginger leaf. Consistent with these findings, GLE showed ABTS radical-scavenging activity in a concentration-dependent manner (Fig. S1) and was rich in polyphenols. HPLC analysis indicated high levels of ferulic acid and rutin. Ferulic acid is a plant-derived phenolic compound commonly found in leaf and legumes [39], and rutin is a plant-derived flavonoid that is both non-toxic and non-oxidizing, which makes it more favorable to use than other flavonoids [40]. Polyphenolic compounds have been reported to protect cells against oxidative stress due to their antioxidant properties, thereby exerting anti-obesity effects. Both ferulic acid and rutin exhibit multiple physiologically active properties, including antioxidant and anti-obesity effects [41, 42]. Previous studies have demonstrated that administration of ferulic acid to high-fat diet-induced obese mice reduced body fat accumulation and body weight, thereby decreasing

the risk of obesity and metabolic syndrome [43, 44]. Rutin has been shown to ameliorate obesity by suppressing adipocyte differentiation and the expression of adipogenesis-related transcription factors, as well as regulating body weight in 3T3-L1 cells and obesity-induced mice. This supports the idea that the bioactive compounds in GLE may exert anti-obesity effects, in part, through their antioxidant properties [45, 46]. The ABTS radical-scavenging result reflects chemical antioxidant capacity and was not interpreted as evidence of intracellular redox modulation.

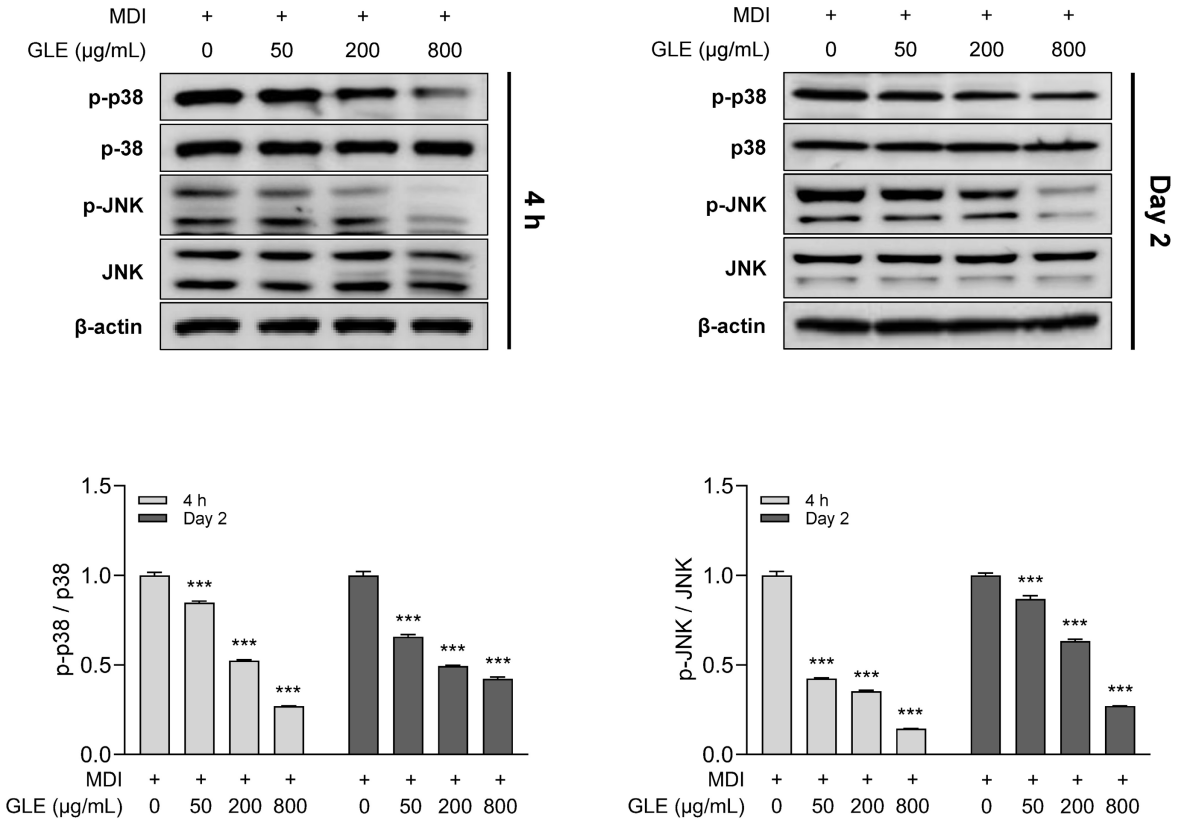

Figure 7. Effects of GLE on MAPK pathway inhibition in 3T3-L1 adipocytes. Western blot images and quantification of p-p38/p38 and p-JNK/JNK at 4 h and day 2. Data are presented as the mean ± SD. ***$p < 0.001$ vs. 0 μg/mL. GLE, ginger leaf subcritical water extract

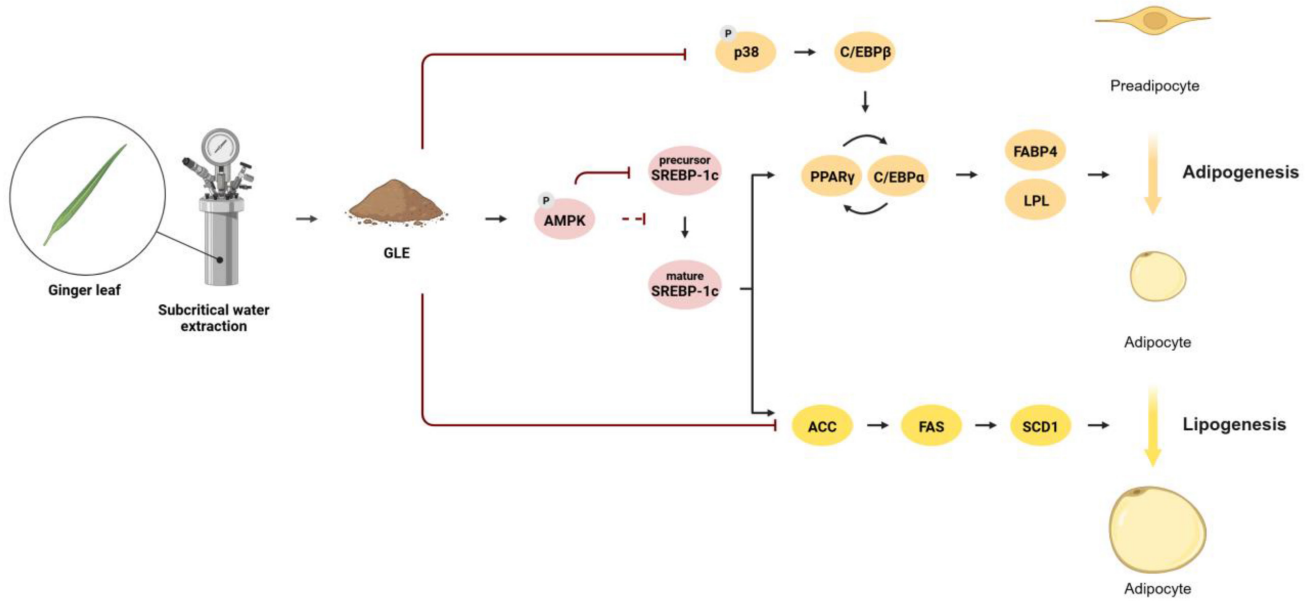

Figure 8. GLE inhibits adipogenesis, lipogenesis, and lipid accumulation through the AMPK–SREBP-1c signaling pathway and regulation of MAPKs

Subcritical water refers to liquid water maintained below its critical temperature (374.15°C) and pressure (22.1 MPa). In this state, it exhibits distinct physicochemical properties that facilitate the dissolution of both polar and nonpolar compounds. Its low viscosity and surface tension, along with a high diffusion coefficient, enhance mass transfer efficiency [47]. Additionally, subcritical water remains relatively stable at elevated temperatures, which helps preserve thermolabile bioactive constituents [48]. Unlike conventional extraction techniques, subcritical water extraction is solvent-free, achieving high extraction efficiency while mitigating solvent-related risks. Despite these advantages, no studies have systematically examined the composition or bioactivities of ginger leaf extracts obtained via subcritical water extraction. In screening, we compared extracts from subcritical water, 70% ethanol, water, and dry powder. Both the water and 70% ethanol extracts showed high cytotoxicity. The dry powder was safe but showed no anti-adipogenic effect. The subcritical water extract was the only one that satisfied both essential criteria: high safety and potent lipid inhibition. Therefore, we selected subcritical water extract for this study (data not shown). In this study, we investigated the anti-obesity potential of GLE by evaluating its effects on adipogenesis and lipogenesis in 3T3-L1 cells and elucidated the mechanisms involved in these processes.

First, we investigated whether GLE affects the differentiation of preadipocytes into adipocytes. C/EBPα functions as a master regulator of adipose tissue development and promotes adipocyte differentiation [38, 49]. Additionally, PPARγ, a transcription factor of the nuclear receptor superfamily, is a key regulator of fat and glucose metabolism and storage [50, 51]. These two critical factors interact during adipogenesis to activate adipogenesis-specific genes, such as FABP4 and LPL [21, 52]. GLE inhibited the expression of C/EBPα, PPARγ, and their downstream targets, FABP4 and LPL, on days 2 and 7 of differentiation. FABP4 is a well-established late adipogenic marker whose expression markedly increases during the later stages of differentiation; therefore, its strong expression on day 7 and the reduction observed with GLE reflect inhibition of late-stage adipocyte maturation. In addition, we hypothesized that GLE reduced the expression of adipogenesis-related genes by initially inhibiting C/EBPβ. C/EBPβ plays a crucial role in MCE and is responsible for the transactivation of the C/EBPα and PPARγ genes [53]. C/EBPβ is expressed immediately after the initiation of adipogenesis, reaching peak levels within 4 h [54]. GLE reduced C/EBPβ expression in 3T3-L1 cells at 4 h, suggesting that GLE inhibits adipogenesis at an early stage.

The MAPK pathway regulates adipogenesis throughout the entire differentiation process [32]. In particular, p38 MAPK promotes adipocyte differentiation by directly activating C/EBPβ during the early stages of differentiation [55]. However, p38 MAPK activity declines after 4 days of differentiation, indicating that its function is primarily restricted to early adipocyte differentiation stages [56]. This temporal specificity suggests that targeting p38 MAPK signaling during early differentiation may be an effective strategy to regulate adipogenesis. Similar to p38, JNK has also been attributed an essential regulatory role limited to the early stages of adipocyte differentiation [57]. We found that GLE inhibited phosphorylation of both p38 and JNK at 4 h and day 2 of differentiation, suggesting that GLE regulates adipogenesis from the outset by targeting the p38–C/EBPβ pathway and JNK. Nevertheless, the role of JNK in adipogenesis remains controversial, warranting further investigation to clarify the mechanisms of JNK activity in adipocytes.

Lipogenesis includes the synthesis of FAs and TGs [58]. FA synthesis is governed by the sequential transcription of ACC, FAS, and SCD1, which are key regulators of lipogenesis [59]. ACC catalyzes the carboxylation of acetyl-CoA to malonyl-CoA, the substrate for FAS. SCD1 catalyzes the conversion of saturated fatty acids (SFAs) into monounsaturated fatty acids (MUFAs), which are essential for the synthesis of TGs, cholesterol esters, and very low-density lipoproteins (VLDL) [60, 61]. In particular, MUFAs are preferentially utilized for TG synthesis compared with SFAs [62, 63]. Therefore, SCD1 plays a key role in lipid metabolism and has been proposed as a potential therapeutic target for obesity. GLE reduced the total ACC expression level and increased ACC phosphorylation. The increase in ACC phosphorylation serves as a short-term off-switch to immediately inactivate the existing ACC enzyme. This is the direct result of AMPK activation [64]. Simultaneously, the decrease in total ACC expression is a long-term machinery reduction. By inhibiting the main adipogenic pathway, such as SREBP-1c [65], GLE reduces the synthesis of new ACC protein. Therefore, GLE provides robust, dual-regulation: it shuts off the enzyme you have via phosphorylation and reduces the expression of the enzyme. GLE also decreased the expression levels of FAS and SCD1. These results suggest that GLE inhibits FA synthesis in 3T3-L1 cells by modulating these key enzymes. Beyond its role in FA synthesis, SCD1 broadly regulates lipid metabolism [63]. A previous study demonstrated that inhibition of SCD1

in adipocytes was linked to activation of AMPK and modulation of SREBP-1c and PPARγ expression [66]. However, the mechanism by which SCD1 influences GLE-induced AMPK activation in 3T3-L1 cells requires further investigation.

The lipid metabolism effects of SREBP-1c have been extensively investigated. SREBP-1c promotes adipogenesis by activating PPARγ ligands [67]. It regulates transcriptional activity by directly binding to the promoters of lipogenic enzymes such as ACC and FAS, and its inhibition improves insulin resistance and reduces lipid accumulation via the FAS/ACC pathway [65, 68]. These findings collectively indicate that SREBP-1c functions as a transcription factor involved in both adipogenesis and lipogenesis. SREBP-1c is synthesized as an inactive precursor in the endoplasmic reticulum (ER), where it forms a complex with SREBP cleavage-activating protein [69]. Its activation requires two sequential proteolytic cleavage steps [70]. The amino-terminal domain of SREBP-1c subsequently translocates to the nucleus, where it induces the expression of genes involved in lipid metabolism. This activation process of SREBP-1c is directly regulated by AMPK. Phosphorylated AMPK binds to the Ser372 residue of SREBP-1c in the ER and phosphorylates SREBP-1c [26, 71]. Phosphorylated SREBP-1c fails to undergo proteolytic cleavage and nuclear translocation, and therefore remains membrane-bound [26]. AMPK phosphorylation is thus considered a master regulatory mechanism in lipid metabolism [72]. In our study, GLE modulated adipogenesis and lipogenesis via the AMPK–SREBP-1c pathway in 3T3-L1 adipocytes. Compound C reversed the effects of GLE on AMPK phosphorylation and mature SREBP-1c expression, indicating that GLE suppressed SREBP-1c activation through AMPK signaling. GLE also reduced precursor SREBP-1c expression, consistent with previous findings that phosphorylated AMPK leads to decreased precursor SREBP-1c levels [71, 73]. These results demonstrate that the AMPK–SREBP-1c pathway plays a key role in the anti-obesity effects of GLE in 3T3-L1 cells. Notably, combined treatment with AICAR, an AMPK activator, and GLE resulted in enhanced anti-obesity effects, suggesting that cooperative activation of AMPK may produce more effective outcomes for obesity treatment. While Compound C robustly suppressed AMPK– SREBP-1c signaling, its effects on adipogenic transcription factors and terminal differentiation markers were partial during the late differentiation stage. This dissociation suggests that AMPK plays a contributory, but not exclusive, role in regulating adipogenesis.

Finally, in our study, GLE significantly inhibited adipogenesis and lipogenesis in a dose-dependent manner (50–800 μg/mL). Notably, the effective starting concentration of GLE (50 μg/mL) was comparable to that reported for ginger rhizome extracts (25–50 μg/mL) in previous studies [74, 75]. Lower concentrations of GLE (up to 200 μg/mL) significantly modulated adipogenic and lipogenic markers, while a strong reduction in lipid accumulation was observed at 800 μg/mL. This suggests that although lower concentrations are sufficient for molecular modulation, a higher concentration is necessary to produce a significant phenotypic effect.

Conclusion

This study demonstrated that GLE inhibits adipogenesis, lipogenesis, and lipid accumulation through the AMPK–SREBP-1c signaling pathway and regulation of MAPKs (Fig. 8). Mechanistically, GLE suppressed the early transcription of adipogenesis- and lipogenesis-related genes at 4 h and day 2 following hormonal induction, with sustained downregulation observed through day 7 of differentiation. These findings highlight the potential of ginger leaf, a byproduct, as a functional ingredient for regulating lipid metabolism. However, further in vivo and clinical studies are required to validate the anti-obesity effects of GLE.

Abbreviations

ABTS: 2,2′-azino-bis(3-ethylbenzothiazoline-6-sulfonic acid); ACC: Acetyl-CoA carboxylase; AMPK: AMP-activated Protein Kinase; ANOVA: Analysis of Variance; C/EBP: CCAAT/enhancer-binding protein; DMEM: Dulbecco's Modified Eagle's Medium; FABP4: Fatty acid binding protein 4; FAS: Fatty acid synthase; FAs: Fatty acids; FBS: Fetal bovine serum; GLE: Ginger leaf subcritical water extract; HPLC: High-performance liquid chromatography; JNK: c-Jun N-terminal kinase; LPL: Lipoprotein lipase; MAPKs: Mitogen-activated protein kinases; MCE: Mitotic clonal expansion; MTT: 3-(4,5-dimethylthiazol-2-yl)-2,5-diphenyltetrazolium bromide; PPARγ: Peroxisome proliferator-activated receptor gamma; SCD1: Stearoyl-CoA desaturase 1; SREBP-1c: Sterol regulatory element-binding protein 1c; TGs: Triglyceride.

Supplementary Material

Supplementary figures.
https://www.medsci.org/v23p2408s1.pdf

Acknowledgements

This study was conducted with the support of the R&D program for Forest Science Technology

(project no. RS-2025-02262982) provided by Korea Forest Service (Korea Forestry Promotion Institute). Figure 8 was created with BioRender.com under license number UM29N50U.

Authorship contribution statement

Eun-Min Jun: Formal analysis, Investigation, Methodology, Validation, Visualization, Writing – original draft. **Jong-Yeon Kim:** Formal analysis, Methodology, Validation. **Jeong-Sook Choe:** Investigation, Methodology. **Eun-Jung Park:** Formal analysis, Conceptualization, Project administration, Supervision, Visualization, Writing – review and editing. **Hae-Jeung Lee:** Conceptualization, Methodology, Funding acquisition, Project administration, Supervision, Writing – review and editing.

Data statement

Data will be made available on request.

Competing Interests

The authors have declared that no competing interest exists.

References

1. Roden M, Shulman GI. The integrative biology of type 2 diabetes. Nature. 2019; 576: 51–60.
2. Rubino F, Cummings DE, Eckel RH, Cohen RV, Wilding JPH, Brown WA, et al. Definition and diagnostic criteria of clinical obesity. Lancet Diabetes Endocrinol. 2025; 13: 221–62.
3. Piche ME, Tchernof A, Despres JP. Obesity Phenotypes, Diabetes, and Cardiovascular Diseases. Circ Res. 2020; 126: 1477–500.
4. Woolford SJ, Sidell M, Li X, Else V, Young DR, Resnicow K, et al. Changes in Body Mass Index Among Children and Adolescents During the COVID-19 Pandemic. JAMA. 2021; 326: 1434–6.
5. Chang TH, Chen YC, Chen WY, Chen CY, Hsu WY, Chou Y, et al. Weight Gain Associated with COVID-19 Lockdown in Children and Adolescents: A Systematic Review and Meta-Analysis. Nutrients. 2021; 13.
6. Han K, Jung JH, Jeong SM, Kim MK. Epidemiology and Trends of Obesity and Bariatric Surgery in Korea. Endocrinol Metab (Seoul). 2024; 39: 678–85.
7. Williams DM, Nawaz A, Evans M. Drug Therapy in Obesity: A Review of Current and Emerging Treatments. Diabetes Ther. 2020; 11: 1199–216.
8. Tak YJ, Lee SY. Long-Term Efficacy and Safety of Anti-Obesity Treatment: Where Do We Stand? Curr Obes Rep. 2021; 10: 14–30.
9. Crichton M, Marshall S, Marx W, Isenring E, Lohning A. Therapeutic health effects of ginger (Zingiber officinale): updated narrative review exploring the mechanisms of action. Nutr Rev. 2023; 81: 1213–24.
10. Ghasemzadeh A, Jaafar HZ, Rahmat A. Identification and concentration of some flavonoid components in Malaysian young ginger (Zingiber officinale Roscoe) varieties by a high performance liquid chromatography method. Molecules. 2010; 15: 6231–43.
11. Tohma H, Gülçin I, Bursal E, Gören AC, Alwasel SH, Köksal E. Antioxidant activity and phenolic compounds of ginger (Zingiber officinale Rosc.) determined by HPLC-MS/MS. J Food Meas Charact. 2017; 11: 556–66.
12. Adebayo-Oyetoro AO, Ogundipe OO, Adeyeye SAO, Akande EA, Akinyele AB. Production and evaluation of tiger nut (Cyperus esculentus) milk flavoured with Moringa oleifera leaf extract. Current Research in Nutrition and Food Science Journal. 2019; 7: 265–71.
13. Akomolafe SF, Atoyebi DA, Ogundare MAB, Akinlua I. Effect of dietary supplementation with raw and boiled ginger (Zingiber officinale Roscoe) rhizome on biochemical parameters of rats fed high cholesterol diet. Nutrire. 2025; 50.
14. Ebrahimzadeh Attari V, Malek Mahdavi A, Javadivala Z, Mahluji S, Zununi Vahed S, Ostadrahimi A. A systematic review of the anti-obesity and weight lowering effect of ginger (Zingiber officinale Roscoe) and its mechanisms of action. Phytother Res. 2018; 32: 577–85.
15. Johnson JB, Batley RJ, Mani JS, du Preez R, Trotter T, Netzel ME, et al. Phytochemical composition and biological activity of native Australian ginger (Alpinia caerulea). J Food Meas Charact. 2024; 18: 2372–84.
16. Chen X, Wang Z, Kan J. Polysaccharides from ginger stems and leaves: Effects of dual and triple frequency ultrasound assisted extraction on structural characteristics and biological activities. Food Bioscience. 2021; 42: 101166.
17. Chang E, Kim CY. Natural Products and Obesity: A Focus on the Regulation of Mitotic Clonal Expansion during Adipogenesis. Molecules. 2019; 24.
18. Guo W, Zhang KM, Tu K, Li YX, Zhu L, Xiao HS, et al. Adipogenesis licensing and execution are disparately linked to cell proliferation. Cell Res. 2009; 19: 216–23.
19. Garin-Shkolnik T, Rudich A, Hotamisligil GS, Rubinstein M. FABP4 attenuates PPARgamma and adipogenesis and is inversely correlated with PPARgamma in adipose tissues. Diabetes. 2014; 63: 900–11.
20. Lee JH, Lee SH, Lee HS, Ji ST, Jung SY, Kim JH, et al. Lnk is an important modulator of insulin-like growth factor-1/Akt/peroxisome proliferator-activated receptor-gamma axis during adipogenesis of mesenchymal stem cells. Korean J Physiol Pharmacol. 2016; 20: 459–66.
21. Gregoire FM, Smas CM, Sul HS. Understanding adipocyte differentiation. Physiol Rev. 1998; 78: 783–809.
22. Shimano H. SREBPs: physiology and pathophysiology of the SREBP family. FEBS J. 2009; 276: 616–21.
23. Shimano H, Sato R. SREBP-regulated lipid metabolism: convergent physiology - divergent pathophysiology. Nat Rev Endocrinol. 2017; 13: 710–30.
24. Horton JD, Goldstein JL, Brown MS. SREBPs: activators of the complete program of cholesterol and fatty acid synthesis in the liver. J Clin Invest. 2002; 109: 1125–31.
25. Hardie DG. Keeping the home fires burning: AMP-activated protein kinase. J R Soc Interface. 2018; 15.
26. Li Y, Xu S, Mihaylova MM, Zheng B, Hou X, Jiang B, et al. AMPK phosphorylates and inhibits SREBP activity to attenuate hepatic steatosis and atherosclerosis in diet-induced insulin-resistant mice. Cell Metab. 2011; 13: 376–88.
27. Fu M, Yoon KS, Ha J, Kang I, Choe W. Crosstalk Between Antioxidants and Adipogenesis: Mechanistic Pathways and Their Roles in Metabolic Health. Antioxidants (Basel). 2025; 14.
28. Guo W, Xie W, Han J. Modulation of adipocyte lipogenesis by octanoate: involvement of reactive oxygen species. Nutr Metab (Lond). 2006; 3: 30.
29. Braud L, Battault S, Meyer G, Nascimento A, Gaillard S, de Sousa G, et al. Antioxidant properties of tea blunt ROS-dependent lipogenesis: beneficial effect on hepatic steatosis in a high fat-high sucrose diet NAFLD obese rat model. J Nutr Biochem. 2017; 40: 95–104.
30. Yamamoto M, Nagasawa Y, Fujimori K. Glycyrrhizic acid suppresses early stage of adipogenesis through repression of MEK/ERK-mediated C/EBPbeta and C/EBPdelta expression in 3T3-L1 cells. Chem Biol Interact. 2021; 346: 109595.
31. Peng H, Lin X, Wang Y, Chen J, Zhao Q, Chen S, et al. Epigallocatechin gallate suppresses mitotic clonal expansion and adipogenic differentiation of preadipocytes through impeding JAK2/STAT3-mediated transcriptional cascades. Phytomedicine. 2024; 129: 155563.
32. Bost F, Aouadi M, Caron L, Binetruy B. The role of MAPKs in adipocyte differentiation and obesity. Biochimie. 2005; 87: 51–6.
33. Kim JY, Park EJ, Lee HJ. Ameliorative Effects of Lactobacillus plantarum HAC01 Lysate on 3T3-L1 Adipocyte Differentiation via AMPK Activation and MAPK Inhibition. Int J Mol Sci. 2022; 23.
34. Bray GA. Medical consequences of obesity. J Clin Endocrinol Metab. 2004; 89: 2583–9.
35. Heindel JJ, Lustig RH, Howard S, Corkey BE. Obesogens: a unifying theory for the global rise in obesity. Int J Obes (Lond). 2024; 48: 449–60.
36. Vermaak I, Viljoen AM, Hamman JH. Natural products in anti-obesity therapy. Nat Prod Rep. 2011; 28: 1493–533.
37. Zhang M, Zhao R, Wang D, Wang L, Zhang Q, Wei S, et al. Ginger (Zingiber officinale Rosc.) and its bioactive components are potential resources for health beneficial agents. Phytother Res. 2021; 35: 711–42.
38. Linhart HG, Ishimura-Oka K, DeMayo F, Kibe T, Repka D, Poindexter B, et al. C/EBPalpha is required for differentiation of white, but not brown, adipose tissue. Proc Natl Acad Sci U S A. 2001; 98: 12532–7.
39. Kumar N, Pruthi V. Potential applications of ferulic acid from natural sources. Biotechnol Rep (Amst). 2014; 4: 86–93.
40. Sharma S, Ali A, Ali J, Sahni JK, Baboota S. Rutin : therapeutic potential and recent advances in drug delivery. Expert Opin Investig Drugs. 2013; 22: 1063–79.
41. Boyle SP, Dobson VL, Duthie SJ, Hinselwood DC, Kyle JA, Collins AR. Bioavailability and efficiency of rutin as an antioxidant: a human supplementation study. Eur J Clin Nutr. 2000; 54: 774–82.
42. Zdunska K, Dana A, Kolodziejczak A, Rotsztejn H. Antioxidant Properties of Ferulic Acid and Its Possible Application. Skin Pharmacol Physiol. 2018; 31: 332–6.
43. Choi I, Park Y, Choi H, Lee EH. Anti-adipogenic activity of rutin in 3T3-L1 cells and mice fed with high-fat diet. Biofactors. 2006; 26: 273–81.
44. de Melo TS, Lima PR, Carvalho KM, Fontenele TM, Solon FR, Tome AR, et al. Ferulic acid lowers body weight and visceral fat accumulation via modulation of enzymatic, hormonal and inflammatory changes in a mouse model of high-fat diet-induced obesity. Braz J Med Biol Res. 2017; 50: e5630.
45. Hosseini B, Saedisomeolia A, Allman-Farinelli M. Association Between Antioxidant Intake/Status and Obesity: a Systematic Review of Observational Studies. Biol Trace Elem Res. 2017; 175: 287–97.

46. Almoraie NM, Shatwan IM. The Potential Effects of Dietary Antioxidants in Obesity: A Comprehensive Review of the Literature. Healthcare (Basel). 2024; 12.
47. Cheng Y, Xue F, Yu S, Du S, Yang Y. Subcritical Water Extraction of Natural Products. Molecules. 2021; 26.
48. Zhang JX, Wen CT, Zhang HH, Duan YQ, Ma HL. Recent advances in the extraction of bioactive compounds with subcritical water: A review. Trends Food Sci Tech. 2020; 95: 183–95.
49. Sarjeant K, Stephens JM. Adipogenesis. Cold Spring Harb Perspect Biol. 2012; 4: a008417.
50. Qiu Y, Gan M, Wang X, Liao T, Chen Q, Lei Y, et al. The global perspective on peroxisome proliferator-activated receptor gamma (PPARgamma) in ectopic fat deposition: A review. Int J Biol Macromol. 2023; 253: 127042.
51. Montaigne D, Butruille L, Staels B. PPAR control of metabolism and cardiovascular functions. Nat Rev Cardiol. 2021; 18: 809–23.
52. Madsen MS, Siersbaek R, Boergesen M, Nielsen R, Mandrup S. Peroxisome proliferator-activated receptor gamma and C/EBPalpha synergistically activate key metabolic adipocyte genes by assisted loading. Mol Cell Biol. 2014; 34: 939–54.
53. Gantt K, Cherry J, Tenney R, Karschner V, Pekala PH. An early event in adipogenesis, the nuclear selection of the CCAAT enhancer-binding protein beta (C/EBPbeta) mRNA by HuR and its translocation to the cytosol. J Biol Chem. 2005; 280: 24768–74.
54. Tang QQ, Lane MD. Activation and centromeric localization of CCAAT/enhancer-binding proteins during the mitotic clonal expansion of adipocyte differentiation. Genes Dev. 1999; 13: 2231–41.
55. Manieri E, Sabio G. Stress kinases in the modulation of metabolism and energy balance. J Mol Endocrinol. 2015; 55: R11–22.
56. Engelman JA, Lisanti MP, Scherer PE. Specific inhibitors of p38 mitogen-activated protein kinase block 3T3-L1 adipogenesis. J Biol Chem. 1998; 273: 32111–20.
57. Kusuyama J, Ohnishi T, Bandow K, Amir MS, Shima K, Semba I, et al. Constitutive activation of p46JNK2 is indispensable for C/EBPdelta induction in the initial stage of adipogenic differentiation. Biochem J. 2017; 474: 3421–37.
58. Kersten S. Mechanisms of nutritional and hormonal regulation of lipogenesis. EMBO Rep. 2001; 2: 282–6.
59. Sampath H, Miyazaki M, Dobrzyn A, Ntambi JM. Stearoyl-CoA desaturase-1 mediates the pro-lipogenic effects of dietary saturated fat. J Biol Chem. 2007; 282: 2483–93.
60. Flowers MT, Ntambi JM. Role of stearoyl-coenzyme A desaturase in regulating lipid metabolism. Curr Opin Lipidol. 2008; 19: 248–56.
61. Cohen P, Friedman JM. Leptin and the control of metabolism: role for stearoyl-CoA desaturase-1 (SCD-1). J Nutr. 2004; 134: 2455S–63S.
62. Miyazaki M, Kim YC, Gray-Keller MP, Attie AD, Ntambi JM. The biosynthesis of hepatic cholesterol esters and triglycerides is impaired in mice with a disruption of the gene for stearoyl-CoA desaturase 1. J Biol Chem. 2000; 275: 30132–8.
63. Dragos SM, Bergeron KF, Desmarais F, Suitor K, Wright DC, Mounier C, et al. Reduced SCD1 activity alters markers of fatty acid reesterification, glyceroneogenesis, and lipolysis in murine white adipose tissue and 3T3-L1 adipocytes. Am J Physiol Cell Physiol. 2017; 313: C295–C304.
64. Liu C, Guo Y, Sun L, Lai X, Li Q, Zhang W, et al. Six types of tea reduce high-fat-diet-induced fat accumulation in mice by increasing lipid metabolism and suppressing inflammation. Food Funct. 2019; 10: 2061–74.
65. Shimomura I, Shimano H, Korn BS, Bashmakov Y, Horton JD. Nuclear sterol regulatory element-binding proteins activate genes responsible for the entire program of unsaturated fatty acid biosynthesis in transgenic mouse liver. J Biol Chem. 1998; 273: 35299–306.
66. Kim E, Lee JH, Ntambi JM, Hyun CK. Inhibition of stearoyl-CoA desaturase1 activates AMPK and exhibits beneficial lipid metabolic effects in vitro. Eur J Pharmacol. 2011; 672: 38–44.
67. Kim EJ, Kang MJ, Seo YB, Nam SW, Kim GD. Acer okamotoanum Nakai Leaf Extract Inhibits Adipogenesis Via Suppressing Expression of PPAR gamma and C/EBP alpha in 3T3-L1 Cells. J Microbiol Biotechnol. 2018; 28: 1645–53.
68. Gong Z, Han S, Li C, Meng T, Huo Y, Liu X, et al. Rhinacanthin C Ameliorates Insulin Resistance and Lipid Accumulation in NAFLD Mice via the AMPK/SIRT1 and SREBP-1c/FAS/ACC Signaling Pathways. Evid Based Complement Alternat Med. 2023; 2023: 6603522.
69. Chandrasekaran P, Weiskirchen R. The Role of SCAP/SREBP as Central Regulators of Lipid Metabolism in Hepatic Steatosis. Int J Mol Sci. 2024; 25.
70. Ferre P, Phan F, Foufelle F. SREBP-1c and lipogenesis in the liver: an update1. Biochem J. 2021; 478: 3723–39.
71. Ha JH, Jang J, Chung SI, Yoon Y. AMPK and SREBP-1c mediate the anti-adipogenic effect of beta-hydroxyisovalerylshikonin. Int J Mol Med. 2016; 37: 816–24.
72. Lian Z, Li Y, Gao J, Qu K, Li J, Hao L, et al. A novel AMPK activator, WS070117, improves lipid metabolism discords in hamsters and HepG2 cells. Lipids Health Dis. 2011; 10: 67.
73. Jang J, Jung Y, Seo SJ, Kim SM, Shim YJ, Cho SH, et al. Berberine activates AMPK to suppress proteolytic processing, nuclear translocation and target DNA binding of SREBP-1c in 3T3-L1 adipocytes. Mol Med Rep. 2017; 15: 4139–47.
74. Li H, Rafie AR, Hamama A, Siddiqui RA. Immature ginger reduces triglyceride accumulation by downregulating Acyl CoA carboxylase and phosphoenolpyruvate carboxykinase-1 genes in 3T3-L1 adipocytes. Food Nutr Res. 2023; 67.
75. Rani MP, Krishna MS, Padmakumari KP, Raghu KG, Sundaresan A. Zingiber officinale extract exhibits antidiabetic potential via modulating glucose uptake, protein glycation and inhibiting adipocyte differentiation: an in vitro study. J Sci Food Agric. 2012; 92: 1948–55.